The post-yield fracture of a ductile polymer film: Notch quality, essential work of fracture, crack tip opening displacement, and J-integral

A.B. Martínez

N. León*

noel.leon@estudiant.upc.edu

D. Arencón

M. Sánchez-Soto

Centre Català del Plàstic, Departament de Ciència dels Materials i Enginyeria Metal-lúrgica, Universitat Politècnica de Catalunya-Barcelona TECH, C/Colom 114, 08222 Terrassa, Spain

*Corresponding author.

Abstract

Double edge notched tension (DENT) specimens of a polyethylene terephthalate (PET) film were tested in an universal testing machine, measuring the displacements and the ligament lengths with a digital image correlation (DIC) system. With these data the essential work of fracture (EWF), crack tip opening displacement (CTOD), and the J-integral fracture methods were compared. The specimens were tested in mode I under plane stress conditions, verifying that the crack always propagated through a fully yielded ligament. It has been proved that w_e, the specific essential work of fracture was the specific energy just up to crack initiation and has the same value that J-integral at crack initiation, J_o. The relationship of these parameters with the CTOD was also shown. The influence of the notch quality on the fracture behaviour when the specimens were sharpened by two different methods, femtosecond laser ablation or by razor blade sliding, has also been analysed in detail.

Keywords: Essential work of fracture; Crack tip opening displacement; J-integral; Polymer film; Femtolaser

Nomenclature

a

crack length

cte

constant

CTOD

crack tip opening displacement

d

displacement

DENT

double edge notched tension specimen

DIC

digital image correlation system

E

elastic modulus

EPBC

ethylene-propylene block copolymer

EPFM

elastic plastic fracture mechanics approach

EWF

essential work of fracture approach

IPZ

inner process zone

J

J-integral

LEFM

linear elastic fracture mechanics approach

OPZ

outer process zone

P

load of tail curves extracted from load records

PET

polyethylene terephthalate

PYFM

post-yield fracture mechanics approach

t

specimen thickness

U

energy dissipated in fracture of the specimen

W

specimen width

Z

specimen height

α

propagation contribution to the extension

β

geometrical shape factor related to the OPZ

ν

poisson’s ratio

$CTOD_c$

CTOD value at the onset of crack propagation

d_i

displacement at the onset of crack initiation

d_r

displacement at specimen rupture

l_i

ligament length measured during the test

l_o

initial ligament length

l_{we}

ligament length at d_i

J_o

J-integral value at crack initiation

r_p

plastic zone radius

w_e

specific work of fracture

W_e

essential work of fracture

w_f

specific total energy

W_f

total energy

w_p

specific non-essential work of fracture

W_p

plastic work or non-essential work of fracture

Δa_b

increment of crack length at blunting

σ_{fs}

engineering flow stress

σ_i

stress at the onset of crack initiation

σ_n

nominal stress

σ_y

uniaxial tensile yield stress

1 Introduction

The ability of polymers to be shaped in practically any form makes possible to obtain films which are mainly used in the packaging and agriculture market segments that accounts for a 39.6% and 4.3% of the plastic global demand, respectively.

The classical tests for determining the mechanical properties of polymer films are well established and standardized, but this is not the case for the fracture properties.

The linear elastic fracture mechanics (LEFM) approach is used to study fractures occurring at nominal stresses well below the material yield stress. The main hypothesis of LEFM considers that the dissipated energy is confined in a small area near the crack tip (small scale yielding), and the fracture is brittle, without extensive deformation.

The LEFM approach is not applicable when the plasticity around the crack tip becomes too large; in those cases the elastic plastic fracture mechanics (EPFM) apply and CTOD and J-integral are appropriate methods to characterize fracture. When the crack propagation occurs through a highly deformed and yielded material then the post-yield fracture mechanics (PYFM) can also be applied and the EWF is the most suitable method. For ductile polymers where crack propagation occurs through a fully yielded ligament, the EWF, the CTOD, and the J-integral are commonly used.

The EWF is gaining acceptance to characterize the plane stress toughness of ductile polymer films in mode I, basically using the double edge notched tension (DENT) configuration. The widespread use of the EWF technique is due to the apparent simple DENT specimen preparation and the simple testing.

The specific work of fracture, w_e, becomes an inherent material parameter only if the ligament fully yields before the crack initiation.

In a previous work [1] carried out on an EPBC (ethylene-propylene block copolymer) material where the ligament was completely yielded before the onset of crack initiation, it was concluded that the specific work of fracture was the energy per unit of ligament area just up to crack initiation, that is, an initiation value. This conclusion drives to the question of whether this value is equivalent to J_o in plane stress conditions, because both parameters have the same physical meaning. According to Mai et al. [2] the essential work of fracture is equivalent to the J-integral at initiation, J_o. Although good numerical agreement has been usually found between w_e and J_o, it is still questioned whether w_e represents or not an initiation value. This equivalence between w_e and J_o has been apparently assumed in several articles either in an explicit manner [3–6], or in an implicit way [7–12]. It should be mentioned that there is only one unique clear evidence that w_e is an initiation value, as has been demonstrated in a previous work on an EPBC film [1].

One of the aims of the present work is to find additional evidence that w_e is an initiation value and therefore study the relationships between w_e, J_o and CTOD. For this reason a polyethylene terephthalate (PET) film, having very different mechanical behaviour than the previously studied EPBC, was used here. Moreover, the fracture toughness parameters have been determined on the same test data and on the same DENT specimens.

Another question which is still pendant in the EWF method are the variations of the w_e values found by different laboratories. Bárány et al. [13] in his review on the EWF summarized the w_e values found by different authors for different polymers. The range for PET films was between 35 and 80 kJ/m^2. Martinez et al. [14] observed significant differences in the w_e values when the specimens were sharpened using the femtosecond laser ablation technique or by the classical razor blade sliding method. The latter providing much higher values than the former one. These differences were explained by the presence of plastically deformed material accumulated at the tip of the razor blade sharpened notches in contrast to the almost negligible plastic deformation existing at the tip of the femtolaser sharpened specimens. The differences in the w_e values were attributed to differences in the notch quality produced. Therefore another aim of this work is to investigate in detail the effect of the notch quality on the fracture behaviour.

2 Background

The common approaches for toughness assessment in ductile polymers includes the J-integral, the crack tip opening displacement, and the essential work of fracture. The theoretical principles and key assumptions of these methods are summarized in the following sections.

2.1 Essential work of fracture

The EWF method was firstly proposed by Cotterell and Reddell [15] after Broberg's work on stable crack growth [16]. The EWF theory is based on the hypothesis that the total energy, W_f, involved in the ductile fracture of a precracked specimen can be separated in two terms.

$$W_f = W_e + W_p \quad \textbf{(1)}$$

where W_e, the essential work of fracture, accounts for the energy necessary to generate new crack surfaces while W_p is called the plastic work or the non-essential work of fracture and includes all the other components of energy dissipated in the fracture process.

The EWF concept establishes that the process zone can be divided into an inner process zone (IPZ) where the fracture process actually occurs and an outer process zone (OPZ) (Fig. 1). Thus, W_e is proportional to the IPZ area while W_p is proportional to the volume of the OPZ. Using these considerations, Eq. (1) can be rewritten in specific terms as follows

$$w_f = \frac{W_f}{l_o.t} = w_e + \beta w_p.l_o \quad \textbf{(2)}$$

where l_o is the ligament length, t is the specimen thickness and β is a factor related to the shape of the OPZ.

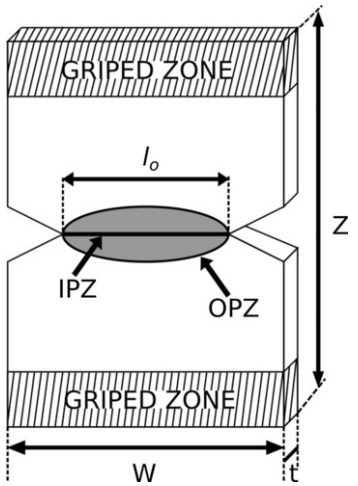

Fig. 1 DENT specimen geometry.

It is possible to assess Eq. (2) by performing a series of tests on DENT specimens with different ligament lengths and plotting the specific total work of fracture, w_f, values as a function of their ligament lengths. A simple linear regression analysis of this plot shows that the specific essential work of fracture, w_e, and the specific non-essential work of fracture, βw_p, are the intercept for a zero ligament length and the slope of the linear regression line, respectively. References [13,17] contain a detailed description of the EWF methodology.

In the EWF analysis the following key assumptions are taken:

(a) The ligament length is fully yielded prior to the onset of crack propagation. Full ligament yielding must show a load drop in the related load-displacement curves [13,18]. This requirement ensures that the fracture mechanism is the same irrespective of the ligament length. However, this key assumption is rarely accomplished and in most of the published articles this requirement is not satisfied and thus the w_e values become an apparent toughness only useful for comparison purposes.

Plane stress conditions and full ligament yielding prior to the crack initiation are accomplished if the following equation is fulfilled.

$$l_o < 2r_p \tag{3}$$

where r_p is the plastic zone radius and can be obtained through:

$$2r_p = \frac{\pi}{8}\left(\frac{Ew_e}{\sigma_y^2}\right) \quad \text{for a linear plastic zone} \tag{4}$$

$$2r_p = \left(\frac{Ew_e}{\pi\sigma_y^2}\right) \quad \text{for a circular plastic zone} \tag{5}$$

where E is the elastic modulus, σ_y is the uniaxial tensile yield stress, and w_e is the specific essential work of fracture.

Although Eq. (3) is a reasonable size criterion, it appears to be too restrictive considering the evidences encountered in amorphous copolyesters [13,18].For pure plane stress conditions, another method is based on the Hill criterion [19–21] but does not ensure full ligament yielding.

(b) Fracture is under plane stress conditions.

In order to meet the plane stress conditions in the specimen ligament length it must be accomplished:

$$l_o \geqslant 3t \text{ or } 5t \tag{6}$$

whereas the condition

$$l_o \leqslant W/3 \tag{7}$$

is necessary to prevent edge effects.

(c) Identical sharp notches without plastic deformation as material volume accumulation at the notch tip, and without thickness increase of the notch root. This requirement [18] guarantees the same value for the crack tip opening displacement at initiation and results in the overlapping of the heads of the nominal stress-displacement and self-similar ligament length-displacement curves for the specimens having different ligament lengths.

The notch sharpening is of crucial importance in obtaining good results. High values of w_e [22] and up to three times higher values of w_e have been reported [23] for razor blade sharpened specimens when the notch tip was blunt or damaged. With razor blade sharpening is easy to generate a volume accumulation of deformed material, at the root of the sharpened notch [14,18,22]. This does not happen with the femtolaser ablated specimens which does not have material volume accumulation at the root of the sharpened notch. The volume accumulation of plastically deformed material is small for low tough polymers and equal w_e values can be obtained for the femtolaser and the razor blade sharpened specimens [18]. However, in the toughest polymers the razor blade sharpening can originate a large volume accumulation of material at the notch root, resulting higher values of w_e compared with the femtolaser sharpened specimens [14].

There are few recent published articles that include the notch tip radii, but in references [14,18,22,24,25] radii less than 5 μm were given. Williams and Rink [23] recommended a notch tip radius equal or lesser than 15 μm,

but decreasing the notch tip radius the w_e value seems to be reduced [22] and a notch tip radius lesser than 5 μm is recommended by us.

2.2 The J-integral

An important concept used in cases of nonlinear elastic behaviour of a crack embedded in a material is the J-integral. Cherepanov [26] and Rice [27] independently developed this concept using a path-independent integral to show a way to calculate the energy release rate per unit area of the crack surface that is created. In simple terms, the J-integral can be expressed as follows

$$J = -\frac{1}{t}\left(\frac{dU}{da}\right)_{d=cte} \quad \textbf{(8)}$$

where U is the energy dissipated in the fracture of the specimen until a given constant displacement, d, and a is the crack length.

There are several approaches for evaluating the J-integral [28] but for the sake of simplicity, the Begley and Landes experimental method [29] will be used here because it can directly be applied to the data registered during the testing of the DENT specimens.

2.3 The crack tip opening displacement, CTOD

Another important fracture mechanics concept first proposed by Wells [30] is the crack tip opening displacement. This method is used to determine a fracture mechanics parameter for ductile materials. It essentially measures the resistance of a material to the propagation of a crack.

Hashemi and O'Brien [11] applied to DENT specimens a method for obtaining the critical crack tip opening displacement $CTOD_c$ (CTOD value at the onset of crack propagation). Under plane stress condition the following linear relationship exists

$$d_r = CTOD_c + \alpha.l_o \quad \textbf{(9)}$$

where d_r is the displacement at rupture and α is the propagation contribution to the displacement. Eq. (9) allows the $CTOD_c$ determination by plotting the displacement at rupture as a function of the ligament length.

The Shih analysis [31] shows that there is a unique relationship between J_o (J value at the onset of crack propagation) and the critical value of the crack tip opening displacement ($CTOD_c$). For a non-hardening material in plane stress and assuming that the stress in the plastic zone is σ_y then

$$J_o = \sigma_y.CTOD_c \quad \textbf{(10)}$$

3 Material and specimen preparation

This study was conducted on a transparent semi-crystalline thermoplastic polyethylene terephthalate (PET) film with low level of crystallinity. The material was kindly supplied by Nudec (Spain) in the form of A4 sheets with a thickness of 0.5 mm.PET is slightly hygroscopic and the sheets have the water absorption at saturation, 0.1–0.2%.

Differential scanning calorimetry (DSC) measurements were conducted on a Q2000 equipment from TA instruments. The samples were heated from 30 to 270 °C at a scanning rate of 10 °C/min. The DSC test revealed a glass transition temperature (T_g) at 73.88 °C, a melting temperature (T_m) at 245.11 °C, and a crystallinity (X_c) of 6.06%.Two kinds of specimens were prepared, dumbbell shaped and DENT specimens.

Dumbbell shaped test specimens were obtained in a cutting press with the shape and dimensions of the type V (ISO 527-3). The deformation behaviour was obtained by testing the dumbbell shaped specimens. The Young's modulus, E, the uniaxial tensile yield stress, σ_y, and the Poisson's ratio, ν, were determined according to the guidelines established in the ISO 527 standard.

The DENT specimens were used to perform the fracture tests. PET films were cut into rectangular coupons 60 mm wide × 90 mm long (Fig. 1). Pre-notches were machined in the rectangular coupons, obtaining samples with different ligament lengths, l_o, varying from 5 to 20 mm. The sharpening of the pre-notches was carried out using two different methods, delivering two sets of DENT specimens to perform fracture testing.

In one set of 20 specimens, the notch sharpening was done through the femtosecond laser ablation. The femtosecond laser used here employs a commercial Ti: sapphire oscillator (Tsunami, Spectra Physics) and is based on the chirped pulse amplification technique. To effectuate the notch sharpening the laser system produced 120 fs pulses around 795 nm at a repetition rate of 1 kHz. The scanning speed was set to 130 μm/s with a pulse energy of 0.07 mJ and 8 passes of the laser beam.

The high-intensity femtosecond laser pulses directly transform the polymer material from the solid phase to the vapour/plasma phase (ablation process) with little heat transfer and avoiding melted and

deformed material at the root of the notch tip. In this manner the local plastic deformation generated at the crack tip is practically negligible.

The second set of 30 specimens was sharpened by manually sliding a fresh steel razor blade across of the machined pre-notch, as the usual generalized way to sharpen polymer film specimens. Only one pass of the razor blade was applied in order to assure that the sharpened extension follow the same path. This technique was carried out manually by a highly skilled operator.

4 Experimental details

All tests were carried out in a Zwick servo-hydraulic testing machine fitted with a two camera digital image correlation (DIC) system (GOM, Germany).

The DIC technique requires surfaces with high contrast to avoid image distortion and therefore inaccurate data. Hence, after sharpening and before testing, one surface of each transparent DENT specimen was covered with a thin white coating before being sprayed to obtain black points as required by the DIC system. The tests were performed at 23 ± 1 °C of temperature, and at a crosshead speed of 1 mm/min. To study the deformation behaviour, the strain was measured by the DIC system with the Aramis software (GOM, Germany).

The DENT specimens were loaded in the testing machine until complete failure. Using the DIC system images of each test were recorded for a later study of crack behaviour. Images were also analysed with the Aramis software for measuring the deformation and ligament length evolution during the test event. With the registered loads, displacements and ligament lengths it was possible to apply the EWF, CTOD and J-integral fracture techniques on the same specimens.

Two sets of data were registered, load as a function of displacement, and ligament length as a function of the displacement.

Unfortunately, the large deformation which occurs in the blunting step during the test causes the loss of the sprayed coating at the root of the notch and the strain field at the onset of crack initiation cannot be observed.

5 Results and discussion

5.1 Deformation behaviour

The uniaxial tensile yield stress (σ_y), modulus (E), and the Poisson's ratio (ν) of the PET material were measured on the dumbbell shaped specimens.

The tensile stress-strain curves, represented in Fig. 2, show an extensive amount of plastic deformation. A yield point (maximum load) can be seen where necking starts, followed by a sudden load drop where the neck develops. Afterwards, there is a drawing of the necked region (cold drawing) during which the tensile deformation continued at a constant stress level (engineering flow stress).

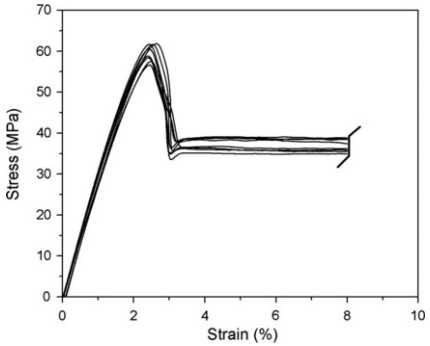

Fig. 2 Uniaxial stress-strain curves.

The results obtained from the tensile test are: E = 2.64 ± 0.02 GPa, σ_y = 58.61 ± 2.05 MPa, σ_{fs} (engineering flow stress) = 37.37 ± 1.48 MPa, and ν = 0.40 ± 0.01.

5.2 Notch quality

In one set of DENT specimens the machined pre-notch was extended by the application of the non-contact femtosecond laser ablation technique. The sharpened notches of three specimens were observed in a scanning electron

microscope (SEM). All the SEM micrographs were similar to the image shown in Fig. 3, having an average sharpening extension of 300 μm and a crack tip radius of 1 μm, both values showing very small deviations. Negligible thermal damage and plastic deformation at the crack tip was observed.

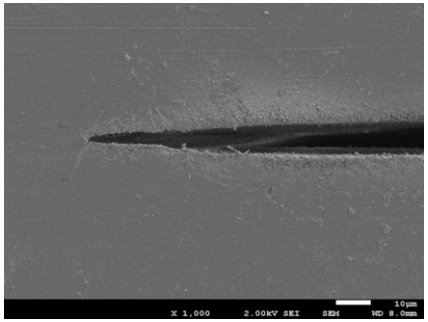

Fig. 3 SEM micrograph of femtolaser sharpened notch.

In the second set of DENT specimens, the pre-notch was extended by the traditional contact method of sliding a fresh razor blade across the pre-notch tip performed in a single pass. The sharpened notches of three specimens were also observed by SEM. Fig. 4a and b shows the micrographs of the two notches of the same DENT specimen. Although both exhibit some plastic deformation at the notch root, the quality of the two notches is different. In Fig. 4b a small volume accumulation of deformed material at the crack tip induced by the compressive component of the sideways sliding force can be observed whereas this feature is not observed in Fig. 4a. This feature depends on the operator skill during the razor blade sharpening [14,18]. The material volume accumulation seems to be larger for the toughest polymers [14,22]. A rising in the thickness at the notch root is caused by the volume accumulation. In comparison to the femtolaser sharpened notches, the SEM analysis of the razor blade notches yields slightly different sharpening depths and similar crack tip radii, but different levels of plastic deformation. The razor blade sliding sharpening method generates notches of different quality which are strongly dependent on the operator skill.

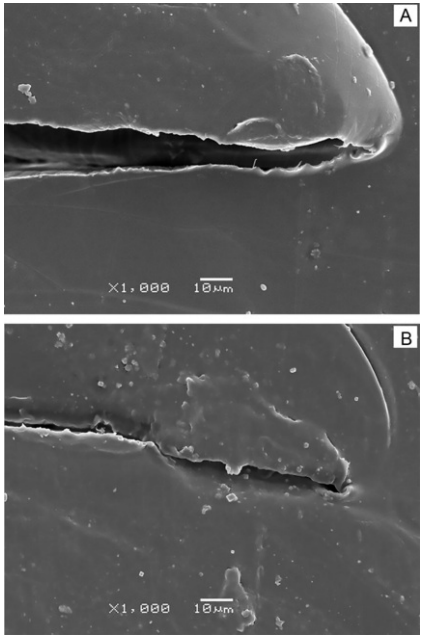

Fig. 4 SEM micrographs of razor blade sharpened notches: (a) Plastic deformation at the crack tip, (b) Plastic accumulation at the crack tip.

The SEM observations of the sharpened notches needed the destruction of the specimens and unfortunately they could not be tested.

5.3 DENT test

Each set of DENT specimens was tested in mode I. The load was registered by the universal testing machine and the displacements by the DIC system. The original ligament lengths, l_o, were measured after testing using an optical microscope. The displacements were obtained by taking as a reference two points closely located to the sharpened notch, and also considering that the OPZ zone must be contained between these two points as shown in Fig. 5.

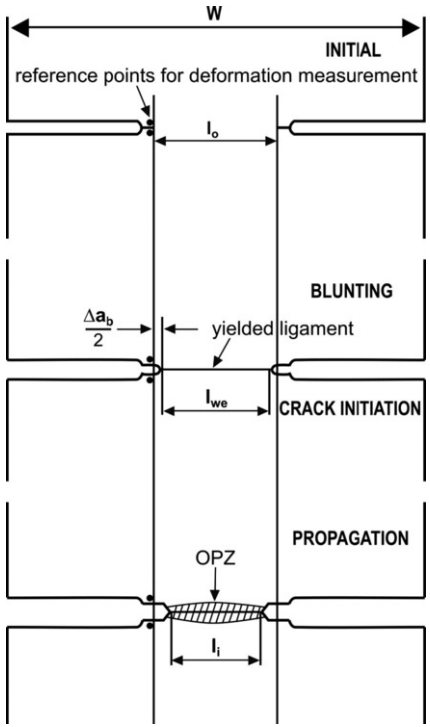

Fig. 5 Scheme of test evolution in a DENT specimen.

The load versus displacement curves are represented in Fig. 6a and b for the femtolaser and for the razor blade sharpened sets of specimens, respectively.

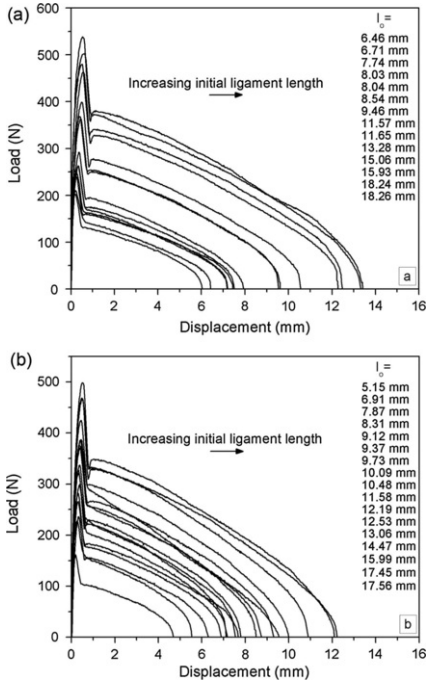

Fig. 6 Load-displacement data: (a) Femtolaser sharpened specimens, (b) Razor blade sharpened specimens.

The frames collected by the DIC system were also processed by the Aramis software and the obtained data of the ligament length as a function of the displacement are represented in Fig. 7a and b.

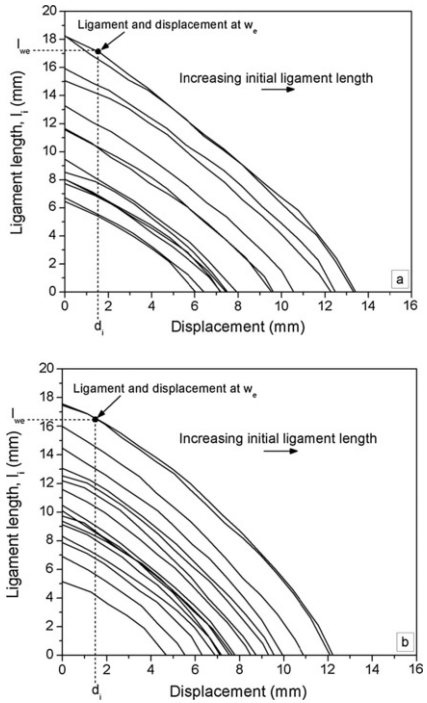

Fig. 7 Tracking of the ligament length during fracture testing: (a) Femtolaser sharpened specimens, (b) Razor blade sharpened specimens.

Of the set of 20 specimens sharpened by femtolaser, 3 specimens were used for SEM observation. The remaining 17 specimens were tested. Figs. 6a and 7a represent the 14 specimens with l_o smaller than $2r_p$.

From the set of 30 specimens sharpened with a razor blade, 3 specimens were used for SEM observation. The remaining 27 specimens were tested, 4 specimens with l_o greater than $2r_p$ were discarded and are not represented in Figs. 6b and 7b. In these figures there are some slightly crossing curves, but we are not able to distinguish between them, these specimens showed the simultaneous crack propagation of both notches.

In other 6 razor blade sharpened specimens the curves load versus displacement and ligament length versus displacement also show crossing curves (do not accomplish self-similarity), for this reason are discarded and are not represented in Figs. 6b and 7b. A careful observation of the frames stored by the DIC system showed that in these 6 razor blade sharpened specimens, the two notches of the same specimen did not propagate simultaneously. This effect is attributed to differences between the two notches. It should be mentioned that this behaviour was not observed in the femtolaser sharpened specimens which exhibited simultaneous crack propagation in both notches.

5.4 Essential work of fracture

The numerical integration of the load-displacement plots of Fig. 6a and b yields the work of fracture, W_f. The specific work of fracture w_f is found when the work of fracture is divided by the area of the original ligament surface. In Fig. 8a and b the specific work of fracture is plotted as a function of the original ligament length by the femtolaser and the razor blade sharpened specimens, respectively. After applying a linear regression, the intercept at the origin gives the w_e value, being βw_p the slope as indicated by Eq. (2).

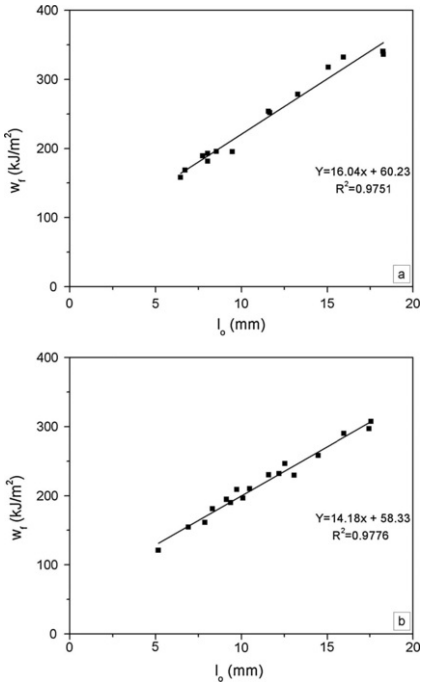

Fig. 8 Essential work of fracture plot: (a) Femtolaser sharpened specimens, (b) Razor blade sharpened specimens.

Once the specific work of fracture, the uniaxial tensile yield stress, and the elastic modulus were obtained, the radius of the plastic zone can be calculated using Eq. (4). From this equation it results $2r_p \approx 18$ mm, so the specimens with ligament lengths larger than 18 mm were eliminated in the data of Figs. 6 and 7 for both sets of sharpened specimens. Since Eqs. (6) and (7) are also accomplished, the key assumptions of the EWF analysis are satisfied. Plane stress conditions and complete ligament yielding prior to the onset of crack growth occurred and thus w_e is an inherent material property. The w_e obtained values of 60.23 and 58.33 kJ/m^2 for femtolaser and razor blade sharpened specimens, respectively; agree well with some of the previous published results [5,32]. Standard errors of the intercepts were 8.90 and 6.55 for the femtolaser and razor blade set of specimens, respectively.

Martinez et al. [1] introduced a new plot which may be useful to clarify the EWF analysis. If the load in Fig. 6 is divided by its initial ligament area, a nominal stress versus displacement, σ_n-d, representation can be obtained. These new plots are represented in Fig. 9a and b for the femtolaser and the razor blade sharpened specimens, respectively. A set of overlapping curves (heads) can be observed in the low displacement range up to a fairly well recognizable displacement value, d_i, from which the curves (tails) start to diverge. The hatched area under the σ_n-d curves is equal to the w_e values of 60.23 and 58.33 kJ/m^2 for the femtolaser and the razor blade sharpened specimens, respectively. This hatched area begins at d = 0 until the displacement d_i, where the crack initiation begins. When the displacements are larger than d_i then there is crack propagation and the curves depart from each other.

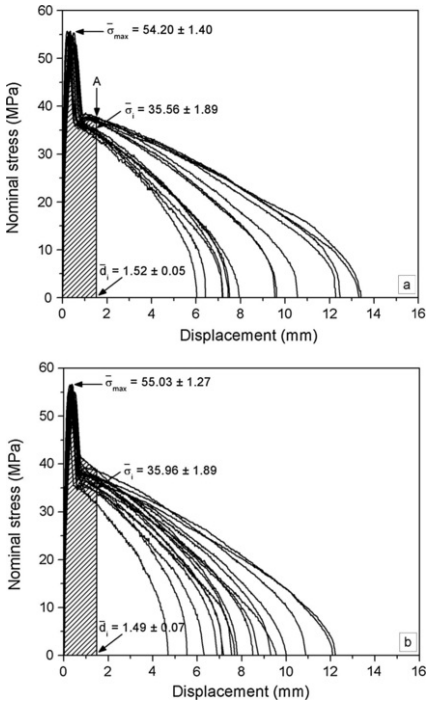

Fig. 9 σ_n – d curves: (a) Femtolaser sharpened specimens, (b) Razor blade sharpened specimens.

From the observation of Fig. 9a and b, the crack initiation displacement d_i, and the crack initiation stress σ_i can be identified. The hatched area represents the specific energy up to crack initiation, and then w_e corresponds to an initiation specific energy. In other words, it represents the energy per surface unit required to create two new surfaces in a cracked body submitted to an external load. An identical behaviour was previously found in other polymer films [1,18].

It is important to remark that the heads of the σ_n-d curves closely resemble those of the uniaxial tensile tests displayed in Fig. 2, including the stress drop characteristic of necking. The average of the maximum nominal stress is basically equal to σ_y and σ_i is also almost equal to the engineering flow stress, σ_{fs}.

In the uniaxial tensile test, curve overlapping occurs if the distance between the displacement reference points is constant for all the specimens and yielding occurs between the above mentioned reference points. The same behaviour is observed for the heads in Fig. 9a and b.

In the DENT tests, the displacements are measured using as a reference two points closely located to the initial sharpened notch and such that the OPZ zone is contained inside. The distance between these reference points was taken constant for all specimens. In this way the elastic and viscoelastic contributions due to the bulk polymer located outside the fracture process are negligible. These contributions affect both the displacements and the energies. The slopes βw_p of the essential work of fracture plots (Fig. 8a and b) are practically identical, 16.04 and 14.18 with standard errors of 0.74 and 0.55 for the femtolaser and razor blade sharpened specimens, respectively. The slopes do not depend of the notch sharpening method, as it has been found in other polymers [1,14,18], but the slope vary when the distance between the displacement reference points is changed [14].

A larger number of tested specimens can reduce the slope and intercept standard errors. More than 20 specimens have been recommended [23].

In Fig. 5 the sequence of events leading to the fracture of the DENT specimens are schematized. The process begins with the opening and blunting of the notch and the yielding and necking of the ligament area, followed by crack initiation and propagation until complete fracture. Prior to crack initiation onset there is an increment of the crack length Δa_b due to blunting, being l_{we} the remaining ligament length to be fractured.

The frame shown in Fig. 10, which represents point A in Fig. 9a is clearly indicative of full ligament yielding before crack initiation. The plastic zone is wedge-shaped and very narrow, which is consistent with a linear plastic zone (Eq. (4)). These observations were similar in all valid specimens.

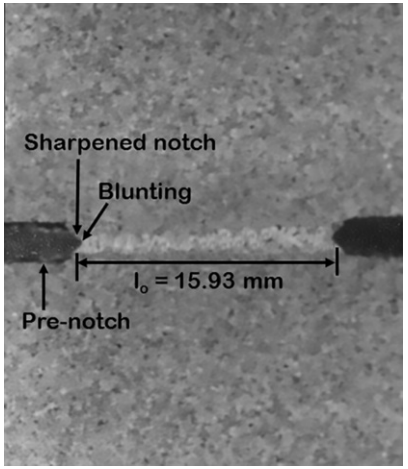

Fig. 10 Frame of a sprayed DENT accounting for the point A in Fig. 9a.

The plastic deformation in front of the crack tip may cause a reduction in w_e because during the crack tip blunting less amount of energy may be necessary. This fact can explain the slightly lesser w_e value obtained for the razor blade sharpened specimens in comparison with the femtolaser one. In tough materials a volume accumulation of plastically deformed material at the crack tip is possible [14] as is shown in Fig. 4b, resulting in a local increase of the crack tip surface. Then if the crack initiates when σ_i is reached, a large local load value will be necessary for those notches having volume accumulation and also d_i will be increased, resulting in a global increase in the fracture energy. This is a plausible explanation for the anomalous behaviour observed in some of the razor blade sharpened specimens that do not show simultaneous propagation of the two notches of the same specimen.

A good way to elucidate the validity of a tested specimen is the observation of the overlapping in the heads of the σ_n-d plot (Fig. 9) and not crossing curves in the ligament length versus displacement plot (Fig. 7). After this analysis, which eliminated the specimens with bad quality notches, the w_e values for both sets of sharpened specimens were virtually identical.

The crack propagation can be analysed as well. When the ligament is completely yielded and necked then

$$P = t(W - a)\sigma_i \tag{11}$$

where P is the load. The derivative yields

$$\frac{dP}{da} = -t\sigma_i \tag{12}$$

then a linear dependence of the load P with the crack length is predicted, being the slope equal to $-t\sigma_i$.

According to Fig. 5 the crack length is

$$a = W - l_i \tag{13}$$

Therefore, combining Figs. 6 and 7 with Eq. (13), it is possible to represent the load as a function of the crack length for the tails, as shown in Fig. 11a for the femtolaser and in Fig. 11b for the razor blade sharpened specimens. In these plots, the linear dependence can be clearly observed and from the slopes the σ_i values of 39.68 and 37.94 MPa are obtained. These values agree well with the σ_i values shown in Fig. 9a and b. All the propagations followed the same trends except at higher crack lengths, close to the complete fracture, where the slope and hence σ_i were found to increase probably as a consequence of orientation hardening. The slopes in Fig. 11a and b correspond to femtolaser and razor blade sets of specimens. This means that the propagation stage does not depend on the notch quality, justifying the equal values found for the slope βw_p in the femtolaser and razor blade sharpened sets of specimens.

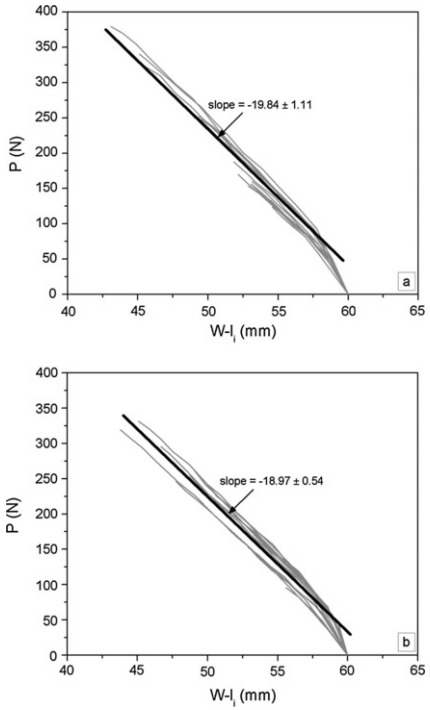

Fig. 11 Tails of load versus crack length: (a) Femtolaser sharpened specimens, (b) Razor blade sharpened specimens.

In Fig. 12 the specific energy versus the crack length for the femtolaser sharpened specimens is represented. The curves are obtained as follows. For each crack length value, a, the corresponding l_i value is obtained (Eq. (13)). For each l_i the corresponding displacement, d, can be found in Fig. 7a. Finally the specific energy is obtained by numerical integration of the curves shown in Fig. 9a up to the above mentioned displacement d. This procedure is repeated for increasing a values and for each specimen.

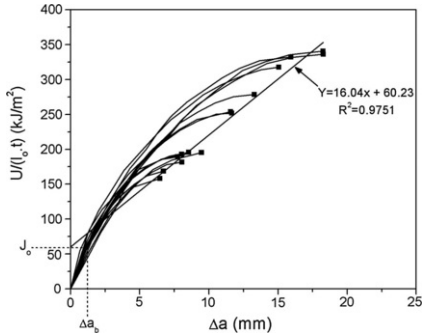

Fig. 12 Specific energy as a function of the crack length for femtolaser set of specimens.

In Fig. 12 it can be observed that there is not a unique curve but the termination points indicate a linear dependence with l_o. In the termination points, l_o is equivalent to Δa at complete fracture. The regression line is the same which was found in the EWF plot (Fig. 8a).

The crack length increment due to blunting just prior to crack initiation (Fig. 5) is given by

$$\Delta a_b = l_o - l_{we} \quad \textbf{(14)}$$

when representing l_{we} as a function of l_o a linear dependence exists. The intercept is $-\Delta a_b$ and the slope is equal to 1. From the l_{we} values taken from Fig. 7a and b, the plots of l_{we} versus l_o are represented in Fig. 13a and b for the femtolaser and the razor blade sharpened specimens, respectively. Both sets of specimens had a slope of 1 and the Δa_b values were 1.15 and 1.23 mm.

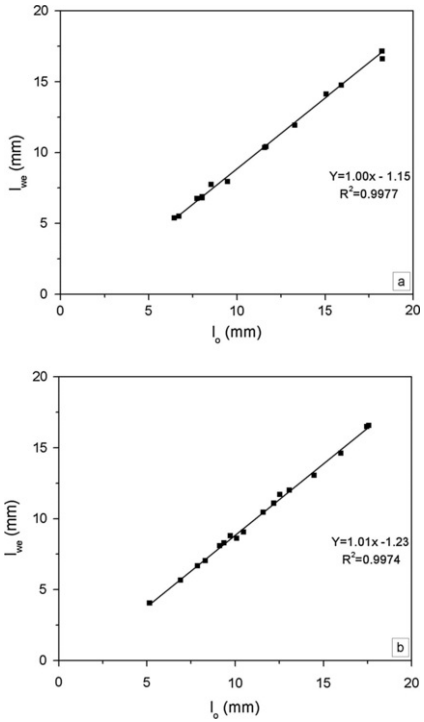

Fig. 13 Determination of the crack length at blunting: (a) Femtolaser sharpened specimens, (b) Razor blade sharpened specimens.

If the increment of crack length just prior to crack initiation Δa_b is introduced in Fig. 12, a coincidence between the specific initiation energy and w_e is again found.

5.5 Crack tip opening displacement

In DENT specimens under plane stress conditions, the critical value of the crack tip opening displacement, $CTOD_c$, that is the CTOD value at initiation has been identified [2,11,33] as the intercept of the linear relationship between the displacement at rupture, d_r, and the original ligament length l_o (Eq. (9)).

Eq. (9) is only valid when there is no displacement contribution of the outside part of the OPZ zone.

Fig. 14a and b shows the displacements at rupture versus l_o for the femtolaser and razor blade sharpened specimens. Clearly there is a linear relationship in the plots, resulting in a $CTOD_c$ value of 1.50 mm for both sets of specimens, which as expected is coincident with the d_i values shown in Fig. 9a and b.

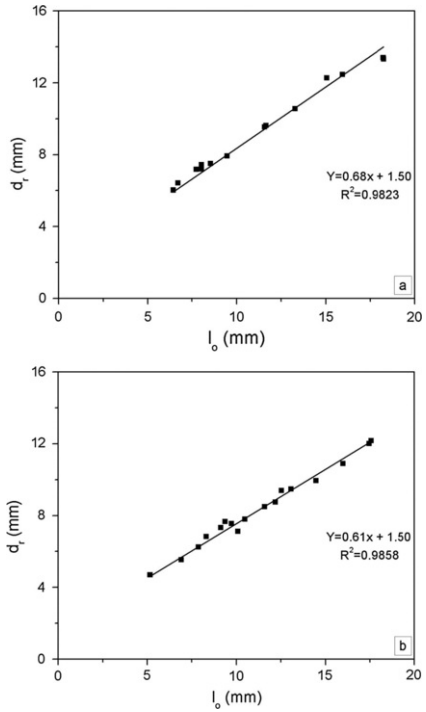

Fig. 14 Displacement at rupture versus l_o: (a) Femtolaser sharpened specimens, (b) Razor blade sharpened specimens.

5.6 J-integral

The Begley and Landes [29] method for the determination of the J-integral is based on Eq. (8) and requires graphical assessment of dU/tda at a constant displacement.

This experimental method is divided in two steps. The first step consists of the graphical representation of the energy divided by the specimen thickness as a function of the crack length at a fixed displacement. The method consists of taking a constant displacement value d, in Fig. 7, where a unique l_i value is found for each specimen. By using Eq. (13) each l_i value is transformed into a crack length value. The energy U is found by numerical integration of the load up to the selected constant displacement value d in Fig. 6. The process is repeated by the adequate selection of new displacements. This graphical representation is shown in Fig. 15a and b for both sets of specimens. The points belonging to the same displacement show linearity and can be fitted by a straight line. Following Eq. (8) the resultant slope from the regression line is –J.

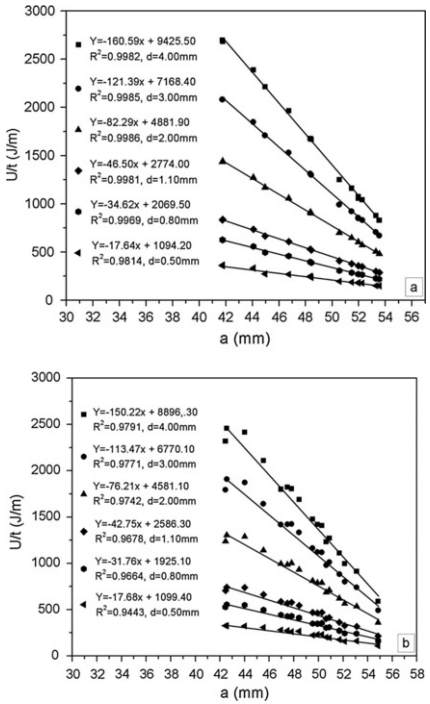

Fig. 15 Input energy divided by thickness versus crack length: (a) Femtolaser sharpened specimens, (b) Razor blade sharpened specimens.

The second step consists of the representation of the J values versus displacement as illustrated in Fig. 16a and b for both set of specimens.

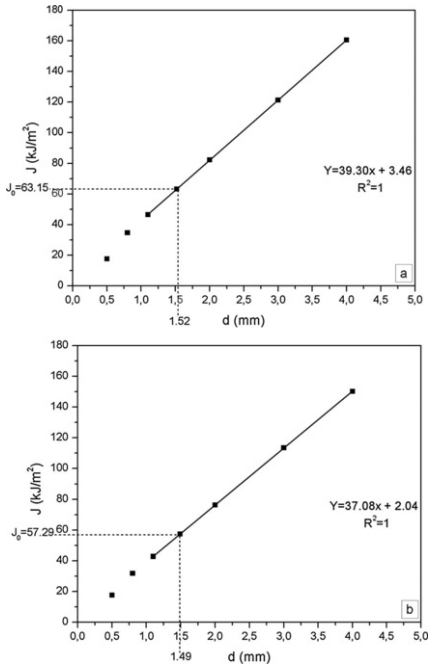

Fig. 16 J-integral: (a) Femtolaser sharpened specimens, (b) Razor blade sharpened specimens.

Following Hodgkinson and Williams [34], the total energy U for a non-work hardening full yielding of the ligament is

$$U = P.d \tag{15}$$

which combined with Eq. (11) results in

$$U = t(W - a)\sigma_i.d \tag{16}$$

U/t is thus a linear function with the crack length at a constant fixed displacement, and is verified in Fig. 15a and b.

If Eq. (8) is combined with Eq. (16) the following expression is obtained

$$J = -\frac{1}{t}\left(\frac{dU}{da}\right)_{d=cte} = \sigma_i.d \tag{17}$$

From the slopes of the regression lines in Fig. 15a and b, and from the slopes in Fig. 16a and b, the verification of Eq. (17) for both sets of specimens is confirmed. The σ_i results match reasonably well with the σ_i values obtained before, taking into account the experimental variability and the involved large data treatment.

The J value at crack initiation, J_o, is obtained by introducing the $CTOD_c$ in the J-integral curves as shown in Fig. 16. The resulting values of 63.15 and 57.29 kJ/m^2 match well with the w_e values of 60.23 and 58.33 kJ/m^2 for the femtolaser and razor blade sharpened specimens, respectively.

Eq. (10) shows the relationship between J_o and $CTOD_c$. In a completely yielded and necked material the stress in the plastic zone is σ_i, then Eq. (10) should be modified as follows

$$J_o = \sigma_i.CTOD_c \tag{18}$$

In the present study this relationship is completely fulfilled. Moreover, our analysis shows a complete relation between w_e, J_o, and $CTOD_c$.

6 Conclusions

In this work it has been demonstrated that the quality of the notches has a strong influence on the repeatability of the DENT fracture test. Main reason justifying different behaviour between razor blade sharpened specimens is the plastic accumulation of material at the crack tip, resulting in a higher w_e if these specimens are not discarded. Moreover, the razor blade sharpening of the specimens causes differences in the quality of notches in the same or between different specimens, resulting in a loss of the self-similarity in both the load and the ligament length versus displacement curves. These differences are most noticeable in the toughest materials where it is easier to generate a large accumulation of deformed material, which results in a rise of the thickness at the crack tip. Different operators can yield different levels of material volume accumulation at the notch tip and this is the decisive factor for the scatter and for the reproducibility. Plotting (σ_n-d) and (l_i-d) could be an appealing way for eliminating the specimens having anomalous behaviour due to their poor notch quality.

The femtosecond ablation laser technique generates repeatable sharp notches, with similar extensions and notch tip radius without plastic deformation, resulting more adequate than the razor blade sliding technique, especially for the fracture study of the toughest polymer films.

The use of the DIC system has allowed the successful application of the EWF, CTOD, and J-integral techniques over a unique set of specimens, resulting in a complete relationship between w_e, J_o, and $CTOD_c$.

In this work on the fracture of a PET film, it is demonstrated that w_e is the energy per unit ligament surface just up to crack initiation, that is, an initiation value. The w_e and J_o values are coincident and it is confirmed that w_e is equivalent with J_o in plane stress when the ligament is completely yielded before the crack initiation onset. w_e and J_o have the same conceptual meaning and are inherent material properties. This is not the case for materials where the ligament is not completely yielded before the crack initiation onset.

Acknowledgements

Authors acknowledge to Ministerio de Economia y Competitividad of Spain for their financial support through the project MAT2012-37762-C02-01. N. León expresses his gratitude to the National Council for Science and Technology (CONACYT) based in Mexico for the doctoral fellowship.

References

[1] A.B. Martínez, A. Segovia, J. Gamez-Perez and M.L. Maspoch, Essential work of fracture analysis of the tearing of a ductile polymer film, *Eng Fract Mech* **77**, 2010, 2654–2661.

[2] Y.W. Mai and P. Powell, Essential work of fracture and j-integral measurements for ductile polymers, *J Polym Sci B Polym Phys* **29**, 1991, 785–793.

[3] Y.W. Mai and B. Cotterell, On the essential work of ductile fracture in polymers, *Int J Fract* **32**, 1986, 105–125.

[4] G. Levita, L. Parisi, A. Marchetti and L. Bartolommei, Effects of thickness on the specific essential work of fracture of rigid PVC, *Polym Eng Sci* **36**, 1996, 2534–2541.

[5] A. Arkhireyeva and S. Hashemi, Determination of fracture toughness of poly (ethylene terephthalate) film by essential work of fracture and J integral measurements, *Plast Rubber Compos* **30**, 2001, 337–350.

[6] A. Arkhireyeva and S. Hashemi, Fracture behaviour of polyethylene naphthalate (PEN), *Polymer* **43**, 2002, 289–300.

[7] A. Arkhireyeva and S. Hashemi, Combined effect of temperature and thickness on work of fracture parameters of unplasticized PVC film, *Polym Eng Sci* **42**, 2002, 504–518.

[8] G. Levita, L. Parisi and S. Mcloughlin, Essential work of fracture in polymer films, *J Mater Sci* **31**, 1996, 1545–1553.

[9] D.E. Mouzakis, J. Karger-Kocsis and E.J. Moskala, Interrelation between energy partitioned work of fracture parameters and the crack tip opening displacement in amorphous polyester films, *J Mater Sci Lett* **19**, 2000, 1615–1619.

[10] J. Karger-Kocsis and T. Czigány, Strain-rate dependence of the work of fracture response of an amorphous poly (ethylene – naphthalate) (PEN) film, *Polym Eng Sci* **40**, 2000, 1809–1815.

[11] S. Hashemi and D. O'Brien, The essential work of plane-stress ductile fracture of poly (ether – ether ketone) thermoplastic, *J Mater Sci* **28**, 1993, 3977–3982.

[12] A. Arkhireyeva and S. Hashemi, Effect of temperature on fracture properties of an amorphous poly (ethylene terephthalate) (PET) film, *J Mater Sci* **37**, 2002, 3675–3683.

[13] T. Bárány, T. Czigány and J. Karger-Kocsis, Application of the essential work of fracture (EWF) concept for polymers, related blends and composites: a review, *Prog Polym Sci* **35**, 2010, 1257–1287.

[14] A.B. Martínez, A. Segovia, J. Gamez-Perez and M.L. Maspoch, Influence of femtolaser notch sharpening technique in the determination of essential work of fracture (EWF) parameters, *Eng Fract Mech* **76**, 2009,

1247–1254.

[15] B. Cotterell and J.K. Reddel, The essential work of plane stress ductile fracture, *Int J Fract* **13**, 1977, 267–277.

[16] K.B. Broberg, On stable crack growth, *J Mech Phys Solids* **23**, 1975, 215–237.

[17] A.B. Martínez, J. Gamez-Perez, M. Sánchez-Soto, J.I. Velasco, O.O. Santana and M.L. Maspoch, The Essential Work of Fracture (EWF) method. Analyzing the post-yielding fracture mechanics of polymers, *Eng Fail Anal* **16**, 2009, 2604–2617.

[18] A.B. Martínez, N. León, D. Arencón and M. Sánchez-Soto, Essential work of fracture, crack tip opening displacement, and J-integral relationship for a ductile polymer film, *Polym Test* **55**, 2016, 247–256.

[19] R. Hill, On discontinuous plastic states with special reference to localized necking in thin sheets, *J Mech Phys Solids* **1**, 1952, 19–30.

[20] B. Cotterell, T. Pardoen and A.G. Atkins, Measuring toughness and the cohesive stress-displacement relationship by the essential work of fracture concept, *Eng Fract Mech* **72**, 2005, 827–848.

[21] F. Tuba, L. Oláh and P. Nagy, On the valid ligament range of specimens for the essential work of fracture method: the inconsequence of stress criteria, *Eng Fract Mech* **99**, 2013, 349–355.

[22] A. Pegoretti, L. Castellani, L. Franchini, P. Mariani and A. Penati, On the essential work of fracture of linear low-density-polyethylene. I. Precision of the testing method, *Eng Fract Mech* **76**, 2009, 2788–2798.

[23] J.G. Williams and M. Rink, The standardisation of the EWF test, *Eng Fract Mech* **74**, 2007, 1009–1017.

[24] M. Rink, L. Andena and C. Marano, The essential work of fracture in relation to J-integral, *Eng Fract Mech* **127**, 2014, 46–55.

[25] A. Dorigato and A. Pegoretti, Fracture behaviour of linear low density polyethylene-fumed silica nanocomposites, *Eng Fract Mech* **79**, 2012, 213–224.

[26] G.P. Cherepanov, Crack propagation in continuous media, *J Appl Math Mech* **31**, 1967, 476–488.

[27] J.R. Rice, A path independent integral and the approximate analysis of strain concentration by notches and cracks, *J Appl Mech* **35**, 1968, 379–386.

[28] X.K. Zhu and J.A. Joyce, Review of fracture toughness (G, K, J, CTOD, CTOA) testing and standardization, *Eng Fract Mech* **85**, 2012, 1–46.

[29] J.A. Begley and J.D. Landes, The J integral as a fracture criterion. In: Fracture toughness, ASTM STP 514, 1972, American Society for Testing and Materials; Philadelphia, 1–20.

[30] A.A. Wells, Application of fracture mechanics at and beyond general yielding, *Br Weld J* **10**, 1963, 293–306.

[31] C.F. Shih, Relationships between the *J*-integral and the crack opening displacement for stationary and extending cracks, *J Mech Phys Solids* **29**, 1981, 305–326.

[32] A. Arkhireyeva and S. Hashemi, Influence of temperature on plane stress ductile fracture of poly (ethylene terephthalate) film, *Plast Rubber Compos* **30**, 2001, 125–131.

[33] S. Hashemi, Fracture toughness evaluation of ductile polymeric films, *J Mater Sci* **32**, 1997, 1563–1573.

[34] J.M. Hodgkinson and J.G. Williams, J and G_c analysis of the tearing of a highly ductile polymer, *J Mater Sci* **16**, 1981, 50–56.

Highlights

- The notch quality affects the repeatability and reproducibility of the DENT test.
- The femtolaser is the best method for the notch sharpening of polymer films.
- w_e is the specific energy just up to crack initiation.
- It is confirmed the equivalence between J_o and w_e.